

## Conference Paper

# Piezoelectric Resonance Temperature Sensor for Active Fibers

D.R. Kharasov<sup>1</sup>, A.V. Konyashkin<sup>1,2</sup>, and O.A. Ryabusshkin<sup>1,2</sup><sup>1</sup>Moscow Institute of Physics and Technology (State University), Dolgoprudny, Russia<sup>2</sup>Kotelnikov Institute of Radioengineering and Electronics (IRE) of Russian Academy of Sciences, Fryazino, Russia

## Abstract

A novel method for temperature measurement of active fibers under conditions of lasing and radiation amplification is introduced. This method allows determination of the longitudinal temperature distribution of active fibers at different optical pump powers. A piezoelectric resonator made of the quartz crystal in the form of a hollow cylinder is used as a temperature sensor. Investigated segment of the active fiber is put thorough the hole of the resonator. Heating temperature of the resonator is determined by measuring a frequency shift of the piezoelectric resonance, which is preliminary calibrated under uniform heating conditions. In order to evaluate the heating temperature of the investigated fiber segment, the last one was substituted with a copper wire coated with polymer. A copper wire was heated by transmitting an electric current and its temperature was determined by measuring the resistance change. Numerical simulations revealed that the heating temperatures of the active and copper fibers differ by less than 9% at 11 W/m thermal load level. Heat transfer coefficient was evaluated using cooling kinetics and stationary state temperature of the "copper" fiber. Heating temperature of the active fiber of the ytterbium fiber laser was measured at different pump levels (up to 150W).

**Keywords:** optical fiber, active fiber heating, fiber laser, temperature sensor, piezoelectric resonance

Corresponding Author:

D.R. Kharasov  
kharasov@phystech.edu

Received: 28 January 2018

Accepted: 15 March 2018

Published: 25 April 2018

Publishing services provided by  
Knowledge E

© D.R. Kharasov et al. This article is distributed under the terms of the [Creative Commons Attribution License](#), which permits unrestricted use and redistribution provided that the original author and source are credited.

Selection and Peer-review under the responsibility of the PhIO Conference Committee.

## 1. Introduction

Radiation power of modern continuous wave fiber lasers reaches several tens kilowatts for single-mode and one hundred kilowatts for multi-mode lasing regimes respectively. In the process of generation and amplification of the radiation, a fraction of the pump power inevitably converts into heat. The heating of the fiber leads to the changes of the laser operation including such parameters as efficiency, output power, beam quality, and the generation wavelength in the free-running mode [1].

### OPEN ACCESS

The polymer coating plays a crucial role in the heating of the fiber. Thermal destruction of the polymer coating [2] is one of the main limiting factors for further power scaling of fiber lasers. Therefore, it is extremely important to be able to measure the temperature of active fibers in processes of generation and amplification of radiation.

Several contact methods for measuring the temperature of active fibers were proposed [3–5]. However, the temperature at the boundary “polymer coating-sensor” differs from the temperature at the boundary “polymer coating-air”. Temperature of an active fiber core was measured using the Mach-Zehnder interferometer [6], fiber Bragg gratings (FBGs) written inside the investigated active fiber [7], the optical time-domain reflectometer [8]. All these methods require preliminary preparations of the optical fiber, which is not always possible. Therefore, a design of the device for measuring the fiber temperature, which can be used in industry, is still an actual task of science and technology.

## 2. Experimental setup

In order to measure the temperature of active fibers under conditions of generation and amplification of laser radiation, the quartz crystal in the form of a hollow cylinder is used in present work. Dimensions of the crystal are  $\varnothing 5 \times 8$  mm and the diameter of the hole is 1 mm (see Figure 1). A block scheme of the electrical part of the experimental setup is shown in Figure 2. A voltage at certain frequency from a radiofrequency (RF) generator is applied to the capacitor with the quartz resonator placed between its electrodes. An electrical current flowing through the capacitor is determined by measuring a voltage drop across the load resistor  $R$  via the lock-in amplifier. An amplitude and phase of the measured frequency response are shown in Figure 3. A linear slope is governed by the capacitance of the capacitor, which is about 1.0 pF. Notches in the frequency response correspond to the resonances of the crystal eigenmodes with the probe electric field (see Figure 3 insets) [9].

## 3. Results

In the range from 20 °C to 100 °C the piezoelectric resonance frequencies of quartz cylinder linearly depend on temperature in the case of its uniform heating. Figure 4

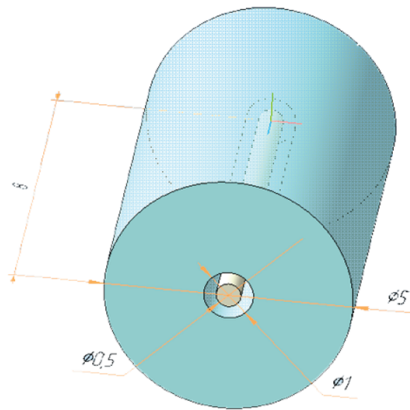


Figure 1: 3D model of the quartz resonator.

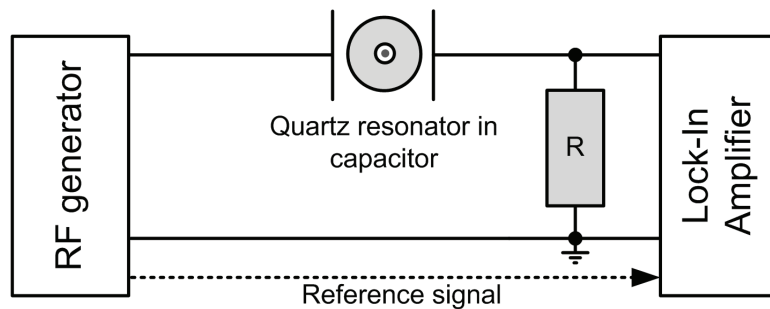


Figure 2: Block-scheme of the experimental setup.

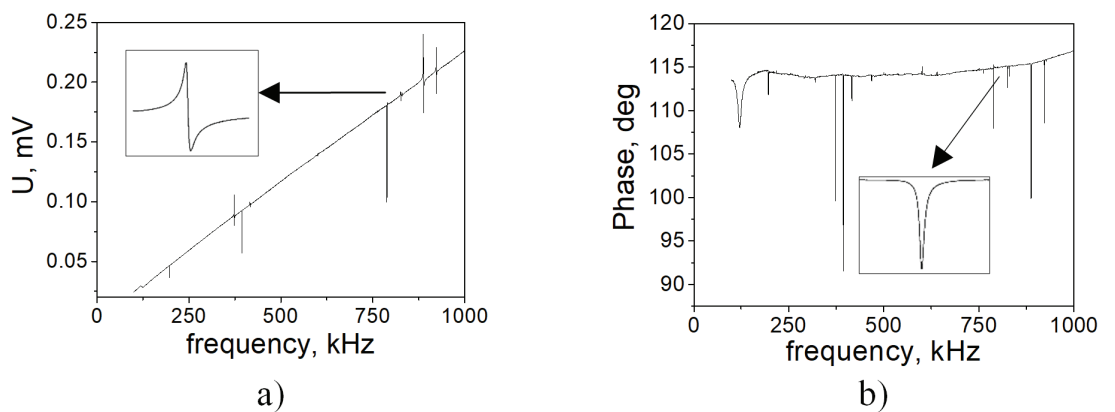


Figure 3: Amplitude (a) and phase (b) of the frequency responses measured on the load resistor R for the quartz resonator.

shows frequency shifts of three resonances at different temperatures. Under nonuniform heating conditions the notion of equivalent temperature  $\theta_{eq}$  is used for determination of piezoelectric resonator temperature[9]:

$$\theta_{eq} = T_0 + \Delta\theta_{eq}, \Delta\theta_{eq} = \frac{\Delta R f}{K_{prt}}. \tag{1}$$

Here  $T_0$ – initial temperature,  $\Delta\theta_{eq}$  – equivalent heating temperature,  $\Delta Rf$ –induced resonance frequency shift,  $K^{prt}$  piezoelectric resonance thermal coefficient measured under conditions of uniform heating.

In order to compare the temperature changes of the quartz resonator  $\Delta\theta_{eq}$  and active fiber  $\Delta T$  a fiber with the copper core and polymer coating is used [5]. Diameters of the copper core and polymer cladding are 250  $\mu\text{m}$  and 400  $\mu\text{m}$  respectively. The fiber is heated by transmitting the DC electric current through it. The temperature of the copper core is evaluated by measuring its resistance. We have measured temperatures of the “copper” fiber fitted through the quartz resonator at different DC current levels (see Figure 5). The relation of slope coefficients measured for the temperatures of the copper wire and quartz resonator is 0.36. It should be noted that the voltage is measured on a relatively long segment of the ‘copper’ fiber (40 cm). Therefore, the resonator, which length is 8 mm, has little effect on the overall measured resistance.

At a current level higher than 5 A, which corresponds to over 100 °C copper core temperature, the polymer coating degradation occurs.

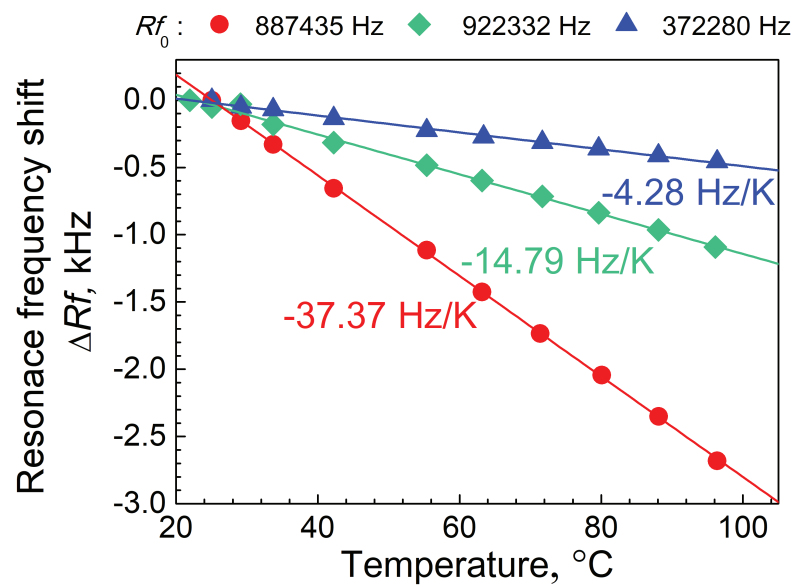
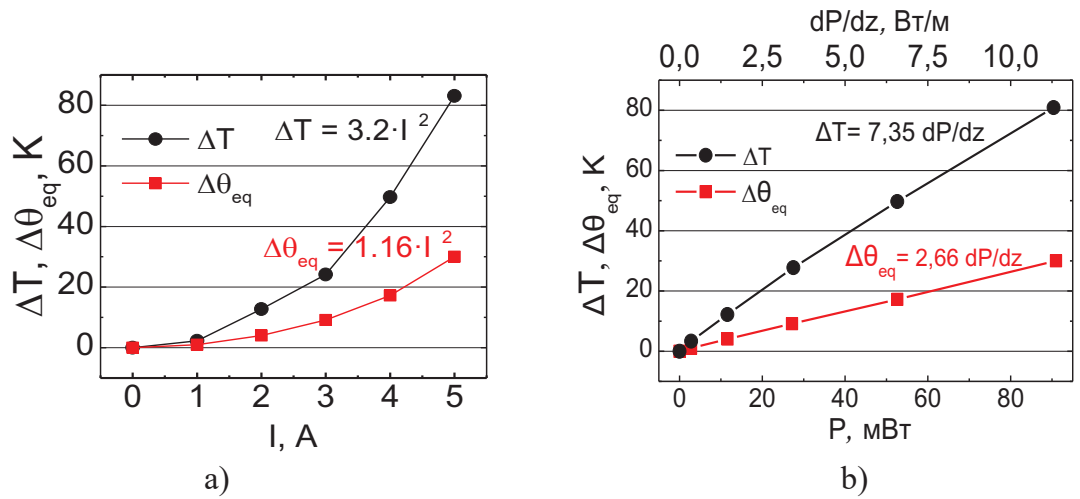


Figure 4: Frequency shift of piezoelectric resonances under uniform heating conditions.

In the case of convective heat exchange with air having temperature  $T_c$ , the temperature at the center of the “copper” fiber  $T_0$  can be obtained[10, 11]:

$$T_0 = T_c + \frac{Qr_{cu}^2}{4k_{cu}} \left[ 1 + 2 \frac{k_{cu}}{k_{pol}} \ln \left( \frac{r_{pol}}{r_{cu}} \right) + \frac{2k_{cu}}{r_{pol}h_T} \right], \quad (2)$$

where  $Q$  – Joule losses density,  $k_{pol} = 1.4 \text{ W/m/K}$ ,  $k_{cu} = 400 \text{ W/m/K}$  – thermal conductivities of the copper and polymer respectively,  $r_{cu}$ ,  $r_{pol}$  – radii of the copper wire



**Figure 5:** Heating temperatures of the copper wire and the quartz resonator at different levels of: a) electric current, b) heat power.

and polymer coating,  $h_T$  – heat transfer coefficient. Dependence of the heat transfer coefficient on the copper core temperature is introduced in Figure 6.

Alternative method for determination of the heat transfer coefficient is based on measuring the cooling kinetics of “copper” fiber after preheating. While “copper” fiber cools, its core temperature  $T$  approaches to the ambient temperature  $T_c$ :

$$T(t) = T_A + (T_0 - T_A) \exp(-t/\tau), \quad \tau = C_P / (h_T S_{surface}), \quad (3)$$

where  $\tau$  – time of the exponential decay,  $S_{surface} = 2\pi \cdot r_{pol} \cdot L$  – surface area,  $C_P = (c_{cu} \rho_{cu} \pi r_{cu}^2 + c_{pol} \rho_{pol} \pi r_{cu}^2) \cdot L$  – heat capacity,  $\rho$  – density,  $c$  – specific heat,  $cu$  – copper,  $pol$  – polymer. Figure 7 shows a block scheme of the experimental setup.

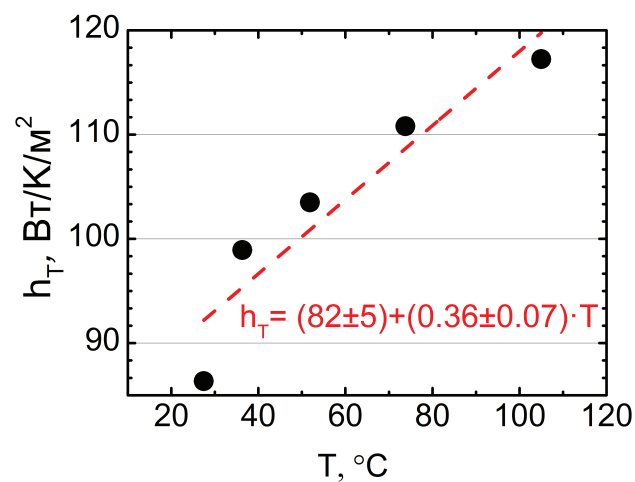


**Figure 6:** Heat transfer coefficient at different temperatures.

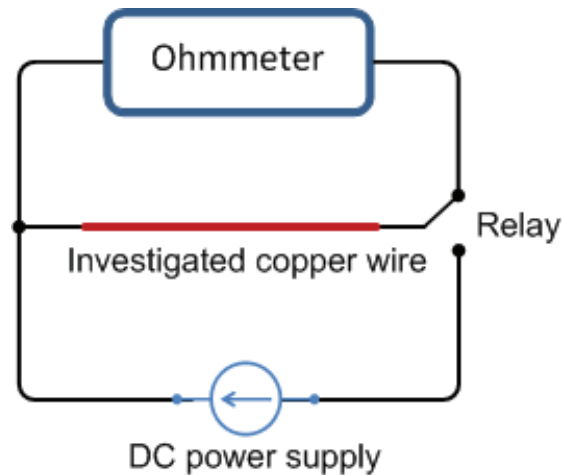


**Figure 7:** Block-scheme of the experimental setup for measurements of cooling kinetics.

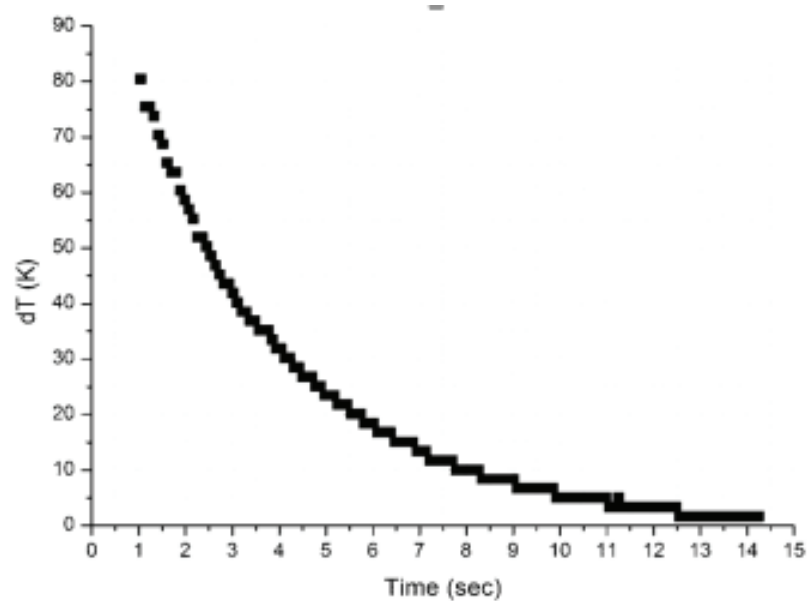


**Figure 8:** Cooling kinetics.

Values of the heat transfer coefficient measured using two different ways do not coincide:  $100 \pm 15 \text{ W/K/m}^2$  and  $70 \pm 3 \text{ W/K/m}^2$  for the first and second method respectively. The possible reason for this is the mismatch of the convective cooling conditions. Since the transverse dimensions of the copper wire coated with polymer coincide with that of active fibers, the measured values can be also used for numerical simulation of the heating and cooling processes of conventional fibers as well as determination of its stationary temperature distribution.

CW ytterbium fiber laser operating at 1063 nm wavelength with 100W output power was assembled. The 13-meters-long GTWave active fiber with 5000 ppm ytterbium

ions concentration was used. It was pumped by seven laser diodes with central wavelength 0.96 μm and maximal total power of 155 W.

Dependence of the heating of the resonator located at the distance of 20 cm from the pump entering point is shown in Figure 9a. The excited-state level population and the pump power longitudinal distribution can be estimated using the rate equation modeling [12]. Heat power generated per unit length at the point z equals to the fraction of absorbed pump radiation multiplied by the percentage of the pump photon energy (quantum defect):

$$\frac{dP}{dz} = \left(1 - \frac{\lambda_p}{\lambda_s}\right) (\sigma_a^p N(z) - \sigma^p N_2(z)) \Gamma_p P_p(z), \quad (4)$$

where  $P_p(z)$  is the pump power at the point z,  $N(z)$  is the concentration of active ions,  $N_2(z)$  is upper state population,  $\sigma_a^p, \sigma^p$  are the absorption and emission cross-sections of Yb ions at the pump wavelength respectively,  $\sigma^p = \sigma_a^p + \sigma^p$ ,  $\Gamma_p$  is the overlapping factor between the pump and the fiber doped area,  $\lambda_p, \lambda_s$  – the pump and signal wavelength. Figure 9b shows heating temperatures in cases of ‘copper’ and conventional active fibers at different heat power levels. The slopes of the linear approximation differ by 25%.

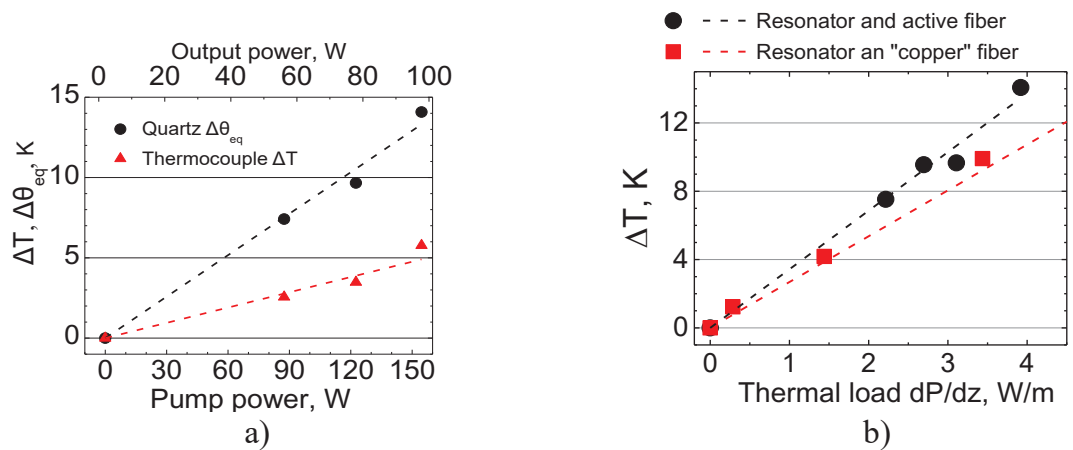


**Figure 9:** a) Resonator heating temperature at different pump levels; b) Resonator heating temperature at heat loads.

The temperature of the active fiber core center can be estimated [10]:

$$T_0 = T_c + \frac{dP}{dz} \frac{1}{4\pi k_F} \left(1 + 2 \ln\left(\frac{r_{clad}}{r_{core}}\right) + 2 \frac{k_F}{k_{pol}} \ln\left(\frac{r_{pol}}{r_{clad}}\right) + 2 \frac{k_F}{r_{pol} h_T}\right), \quad (5)$$

where  $k_F$  – the thermal conductivity of the fused quartz,  $r_{core}, r_{clad}$  – the active core and silica cladding radii. The heat transfer coefficient  $h_T$  of the investigated active fiber is assumed to be equal to that of the “copper” fiber. The heating temperatures of the active fiber (calculated) and the “copper” fiber (measured) coincide within the error limits (see Figure 10).

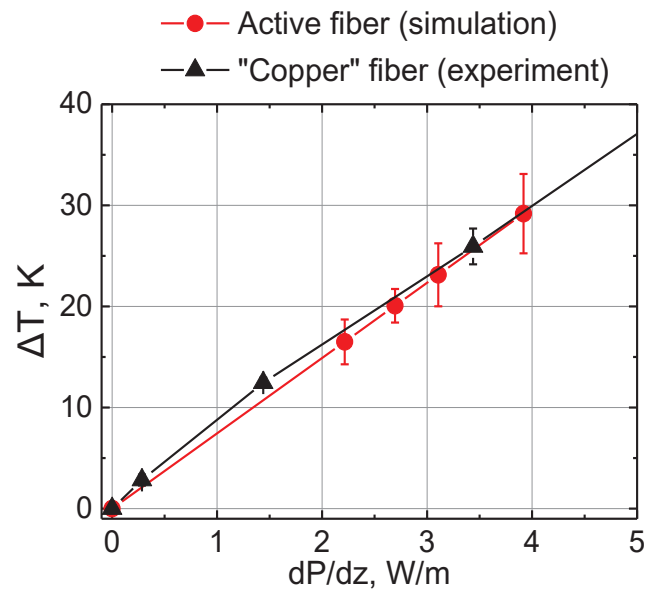


**Figure 10:** Heating temperature of fibers at different heat power level per unit length.

## 4. Discussions

Transverse temperature distributions for "copper" and active (double-clad (DCF) and GTWave) fibers were simulated numerically using the finite element method. Simulation parameters: the heat transfer coefficient  $h_T$  is  $117 \text{ W/K/m}^2$ , the heat power per unit length  $dP/dz$  is  $11 \text{ W/m}$ . This heat power is maximal for the "copper" fiber when no degradation of the polymer coating was observed. The simulation results are presented in Figures 11, 12. Simulation shows that the heating temperatures of GTWave and DCF fiber cores differ by 1.7%. Therefore, the analytical expression (6), which was deduced for a double-clad fiber, can produce relatively good accuracy in the case of GTWave fibers, which have complex geometry. Simulations reveal that the copper core temperature is 9% less comparing with the core temperature of the conventional active fiber. This fact should be taken into account when using 'copper' fibers for the calibration.

Using (2), (5) the optimal radius of the copper core can be evaluated.

Temperature of the copper wire equals to active fiber core temperature, when the radius of the wire is 15-16 times larger comparing with fiber core radius.

It is worth noting that in present configuration the resonator considerably affects the fiber temperature: due to the relatively large ratio of its internal and external diameters, as well as high thermal conductivity of quartz (in comparison with air) as it acts like a radiator. In order to minimize the influence of the resonator on fiber

temperature, it is necessary to reduce the external diameter of the resonator. Nevertheless, the heating temperature of the resonator depends on heat power. In order to perform correct calibration the heating temperature of the 'copper' fiber should also be measured prior to it is putting through the hole of the resonator. It will allow more accurate measurements of the active fiber temperature in lasing conditions.

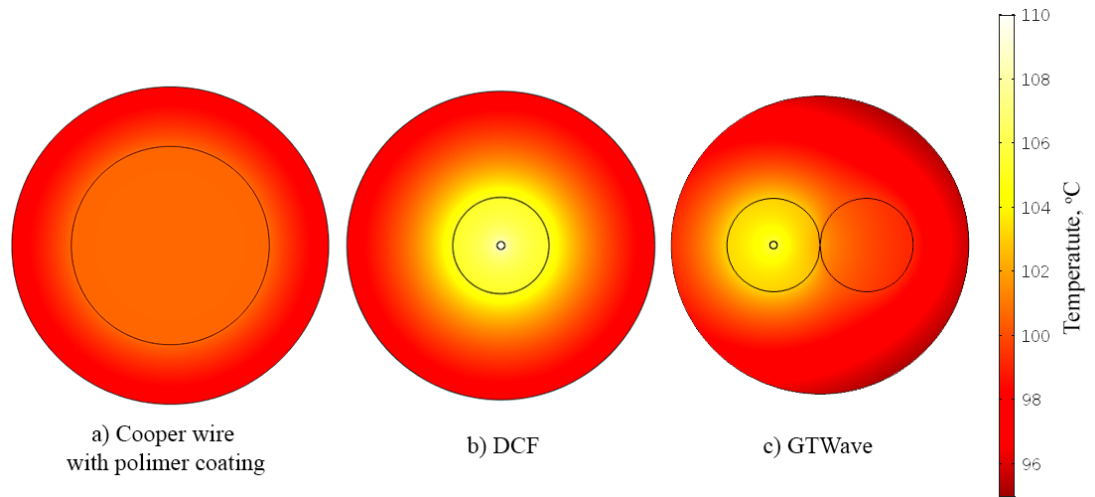


Figure 11: Transverse temperature distribution at heat power 11W/m.

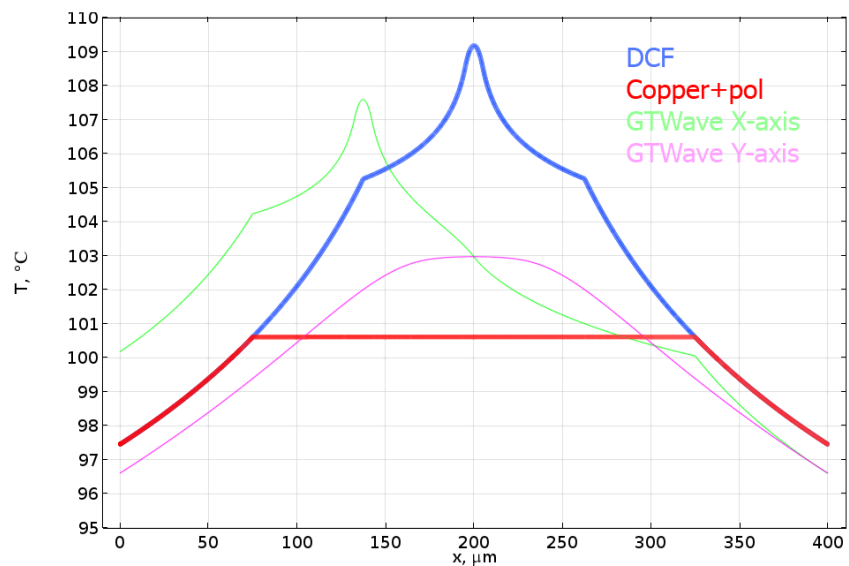


Figure 12: Temperature distribution along radius at heat power 11W/m.

## 5. Conclusions

It was demonstrated that piezoelectric crystals can be used for temperature and heat power measurements. The dependences of the quartz resonator temperature on the

heating temperature of active and “copper” fibers coincide within accuracy of measurements. Thus using a copper wire with polymer coating substituted for an active fiber is expedient for the investigation of the thermal processes occurring inside the fiber and polymer. The degradation of the polymer coating initiated at 95-105 °C in the case of “copper” fiber. A heat transfer coefficient of the “copper” fiber was evaluated using two methods: measuring steady-state temperature at different current levels and measuring cooling kinetics after preheating by an electric current. The temperature sensor design is suitable for measurements of the longitudinal temperature distribution of active fibers under conditions of lasing and amplification. Heating temperature of an ytterbium active fiber was measured in lasing conditions at different pump levels. This method can be used for the development of fiber lasers and its testing.

## Acknowledges

This research was supported by NTO “IRE-Polus”.

## References

- [1] 1. Brilliant N. a, Lagonik K. Thermal effects in a dual-clad ytterbium fiber laser. // Opt. Lett. 2001. Vol. 26, N<sup>o</sup> 21. P. 1669–1671.
- [2] 2. Lapointe M. et al. Thermal Effects in High Power CW Fiber Lasers // Proc. SPIE. 2009. Vol. 7195, N<sup>o</sup> 1. P. 71951U.
- [3] 3. Jeong Y. et al. Thermal characteristics of an end-pumped high-power ytterbium-sensitized erbium-doped fiber laser under natural convection. // Opt. Express. 2008. Vol. 16, N<sup>o</sup> 24. P. 19865–19871.
- [4] 4. Prusakov K., Ryabushkin O., Sypin V. The Longitudinal Temperature Distribution in Active Fibers under Lasing Condition // Advanced Solid State Lasers. Optical Society of America, 2015. P. AM5A.45.
- [5] 5. Ryabushkin O.A., Shaidullin R.I., Zaytsev I.A. Radio-frequency spectroscopy of the active fiber heating under condition of high-power lasing generation // Opt Lett. 2015. Vol. 40, N<sup>o</sup> 9. P. 1972–1975.
- [6] 6. Gainov V. V, Shaidullin R.I., Ryabushkin O.A. Steady-state heating of active fibres under optical pumping // Quantum Electron. 2011. Vol. 41, N<sup>o</sup> 7. P. 637–643.
- [7] 7. Fiebrandt J. et al. In-fiber temperature measurement during optical pumping of Yb-doped laser fibers. 2012. Vol. 8426. P. 84260B.

- [8] 8. Walbaum T. et al. Spatially resolved measurement of the core temperature in a high-power thulium fiber system / ed. Ballato J. 2016. P. 97280P.
- [9] 9. Pigarev A. V, Konyashkin A. V, Ryabushkin O.A. Impedance spectroscopy for measuring low optical absorption coefficients of nonlinear optical crystals // SPIE Photonics Europe. 2016. P. 98941T-98941T.
- [10] 10. Fan Y. et al. Thermal effects in kilowatt all-fiber MOPA // Opt. Express. 2011. Vol. 19, N° 16. P. 15162.
- [11] 11. Brown D.C., Hoffman H.J. Thermal, stress, and thermo-optic effects in high average power double-clad silica fiber lasers // IEEE J. Quantum Electron. 2001. Vol. 37, N° 2. P. 207-217.
- [12] 12. Kelson I., Hardy A. Optimization of strongly pumped fiber lasers // J. Light. Technol. 1999. Vol. 17, N° 5. P. 891-897.